
LARGE LANGUAGE MODEL GUIDED INCENTIVE AWARE REWARD DESIGN FOR COOPERATIVE MULTI-AGENT REINFORCEMENT LEARNING *

Dogan Urgan

Department of Electrical and Electronics Engineering
Karabuk University
78050 Karabuk, Türkiye
durgun@karabuk.edu.tr

Gokhan Gungor

Department of Mechatronics Engineering
Karabuk University
78050 Karabuk, Türkiye
gokhangungor@karabuk.edu.tr

ABSTRACT

Designing effective auxiliary rewards for cooperative multi-agent systems remains a challenging task. Misaligned incentives risk inducing suboptimal coordination, especially when sparse task feedback fails to provide sufficient grounding. This study introduces an automated reward design framework that leverages large language models to synthesize executable reward programs from environment instrumentation. The procedure constrains candidate programs within a formal validity envelope and evaluates their efficacy by training policies from scratch under a fixed computational budget. Selection across generations depends exclusively on the sparse task return. The framework is evaluated across four distinct Overcooked-AI layouts characterized by varied corridor congestion, handoff dependencies, and structural asymmetries. Iterative search generations consistently yield superior task returns and delivery counts, with the most pronounced gains occurring in environments dominated by interaction bottlenecks. Diagnostic analysis of the synthesized shaping components indicates increased interdependence in action selection and improved signal alignment in coordination-intensive tasks. These results demonstrate that the search for objective-grounded reward programs can mitigate the burden of manual engineering while producing shaping signals compatible with cooperative learning under finite budgets.

Keywords Deep learning · large language models · multi-agent learning · reinforcement learning · reward shaping

1 Introduction

The specification of effective reward functions remains a fundamental bottleneck in the deployment of reinforcement learning (RL) systems. While the formal objective of an RL agent is the maximization of a cumulative return, in most complex, high-dimensional domains, the primary task objective is inherently sparse or delayed. This temporal discrepancy creates a severe challenge in credit assignment [1-2], as agents struggle to associate specific exploratory actions with distant positive outcomes. Consequently, the empirical success of modern RL often depends heavily on the manual engineering of auxiliary feedback commonly referred to as reward shaping rather than relying solely on improvements to the underlying optimization algorithms.

In cooperative multi-agent reinforcement learning (MARL), this challenge is significantly amplified by non-stationarity and the absolute necessity for joint exploration. As multiple agents interact within a shared Markov game [3], auxiliary rewards do not merely accelerate individual learning trajectories; they form the underlying incentive structure that governs emergent coordination. When shaping signals are misspecified, agents often develop brittle or parasitic strategies. They learn to maximize a localized proxy signal, such as hoarding resources or prioritizing subtasks while failing to contribute to the global task return. In coordination-intensive environments like Overcooked-AI [4-5], such

*This work is currently under peer review.

reward pathologies manifest themselves as corridor congestion or synchronization failures, effectively decoupling agent behavior from the global objective.

To mitigate these risks, potential-based reward transformations [6-7] provide a rigorous theoretical safeguard that ensures policy invariance. However, these frameworks do not alleviate the intractable practical burden of manually discovering an effective potential function for a highly dynamic multi-agent environment. Traditional data-driven paradigms, including Inverse Reinforcement Learning (IRL) [8] and Learning from Human Preferences [9], attempt to automate this process by recovering reward functions from expert demonstrations. Yet, in simulation-heavy MARL settings, the overhead of collecting synchronized, high-quality multi-agent demonstrations often proves prohibitive. This creates a critical gap in the literature: the growing need for a scalable, autonomous reward design mechanism capable of discovering effective coordination incentives without intensive human-in-the-loop supervision.

The recent evolution of Large Language Models (LLMs) offers a transformative paradigm for addressing this gap. Using the vast generative priors of transformer architectures [10-11], LLMs have demonstrated remarkable competence in synthesizing executable code from natural language specifications [12]. Recent pioneering frameworks, such as Eureka [13] and Text2Reward [14], have successfully utilized LLMs to propose iteratively refined reward programs through empirical feedback. However, these methods have primarily targeted single-agent benchmarks. Applying autonomous reward generation to cooperative MARL introduces unique vulnerabilities, most notably incentive drift, where generated rewards may inadvertently foster competitive proxy behaviors that dismantle collective coordination.

To address these limitations, we propose an objective-grounded reward search framework specifically tailored for cooperative MARL. Unlike existing heuristic-driven generation methods, our approach treats each LLM-synthesized reward program as a candidate hypothesis that undergoes rigorous validation against the latent sparse task objective. By evaluating these reward candidates through end-to-end training using a fixed Multi-Agent Proximal Policy Optimization (MAPPO) algorithm [15], and selecting them exclusively based on their contribution to the global task return, we ensure that the discovered shaping signals remain tightly coupled to the true environmental goal. This closed-loop verification effectively circumvents the risk of reward hacking [16], significantly reducing the need for domain-specific manual tuning and heuristic engineering.

The primary contributions of this work are threefold. First, we propose a novel closed-loop framework utilizing LLMs for reward program synthesis, which incorporates a formal validity envelope and objective-aligned selection to guarantee robust multi-agent coordination. Second, we conduct a comprehensive empirical evaluation across four distinct Overcooked-AI layouts, where the proposed method consistently achieves superior task returns, higher delivery counts, and improved sample efficiency in comparison to manually engineered baselines. Finally, we introduce a suite of diagnostic metrics including action coupling via normalized mutual information and incentive alignment to quantitatively characterize the influence of synthesized rewards on multi-agent learning dynamics and workload distribution.

2 Related Work

The reduction of reward engineering complexity has been a long-standing objective in the reinforcement learning community. Our research intersects with three primary trajectories: theoretical reward transformations, data-driven reward inference, and programmatic reward generation via LLMs.

2.1 Theoretical Foundations of Reward Shaping and Credit Assignment

Reward shaping was formalized to accelerate learning in environments with sparse feedback without altering the optimal policy. The seminal work by Ng et al. [6] established Potential-Based Reward Shaping (PBRS), mathematically proving that augmenting the environment reward with the discounted difference of a state-potential function preserves policy invariance. This framework was subsequently expanded to encompass state-action potentials [17] and dynamic, time-varying potentials [7].

In multi-agent systems, Devlin and Kudenko [18] demonstrated that PBRS effectively maintains the Nash Equilibria of the underlying Markov game. Concurrently, structural approaches to the multi-agent credit assignment problem, such as COMA [2] and value factorization methods like QMIX [19] and VDN [20], attempt to implicitly distribute global rewards among agents. However, while these theoretical and structural constructs provide robust guarantees against altering the global objective, they remain highly reliant on the presence of a reasonably dense external signal. However, these methods fail to automate the discovery of reward signals required for coordination in sparse, high-dimensional tasks. This leaves the reward design as a labor-intensive manual process that cannot easily capture complex inter-agent dependencies [21].

2.2 Data-Driven Reward Inference

To avoid the limitations of manual engineering, data-driven paradigms attempt to recover the underlying reward functions from external sources. Inverse Reinforcement Learning (IRL) [8-22] extracts a reward signal by analyzing the trajectories of experts, operating under the assumption that the expert acts near-optimally. Similarly, Learning from Human Preferences (RLHF) [9-23] utilizes human-provided pairwise comparisons to model the intended objective iteratively.

Despite their empirical success in single-agent robotics, these methods encounter severe scalability bottlenecks in cooperative MARL. Collecting expert demonstrations for multi-agent coordination is exceptionally challenging, as it necessitates perfectly synchronized behavior from all participants. Furthermore, human preference labels are often noisy or inconsistent when evaluating collective behavior, where isolating a single agent’s contribution to a global success remains ambiguous a core issue in multi-agent credit assignment [24]. Unlike these approaches, which require continuous human-in-the-loop supervision, our framework targets an autonomous, simulation-driven discovery process.

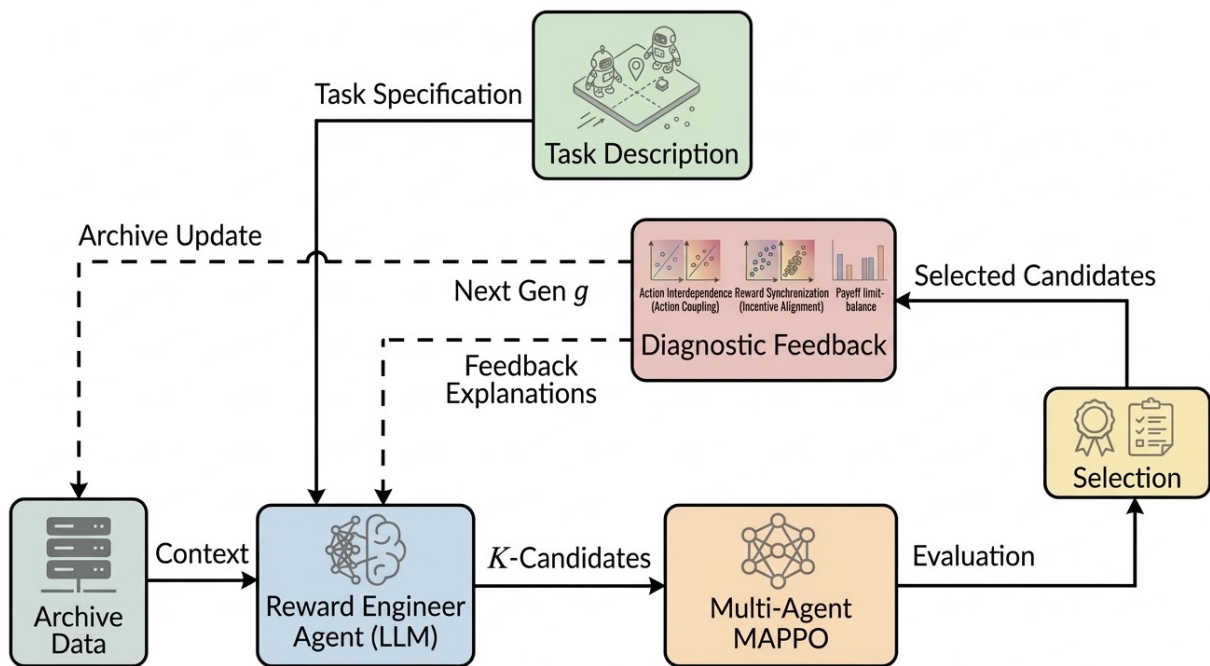


Figure 1: Overview of the proposed autonomous reward search framework. The system establishes a closed-loop optimization process where an LLM-based reward engineer agent iteratively refines reward candidates based on MAPPO evaluations and diagnostic feedback, grounded in task specifications and archive data.

2.3 LLMs for Automated Reward Synthesis and Optimization

The integration of LLMs for code and reward synthesis represents a paradigm shift in automated RL design. Using the advanced reasoning capabilities of pretrained transformers [10-11], recent research treats reward design as a programmatic synthesis task. The concept of utilizing LLMs as meta-optimizers has been firmly established by frameworks like OPRO [25], which demonstrated that language models can iteratively improve solutions based on performance trajectories described in the text. Building on this, the Eureka framework [13] showed that LLMs can achieve human-level reward design for complex robotic tasks by iteratively refining executable Python code based on training logs. Similarly, Text2Reward [14] maps dense natural language instructions directly to executable reward programs. Furthermore, frameworks like Motif [26] have explored using LLMs to provide intrinsic motivation through artificial intelligence feedback.

However, existing LLM-based reward generation frameworks have predominantly focused on single-agent environments or parallel multi-agent tasks where deep coordination is not the primary bottleneck. In environments characterized

by tight interaction bottlenecks (e.g., Overcooked-AI), simply optimizing for individual locomotion often leads to arbitrary conventions that fail to generalize, a challenge heavily documented in the Zero-Shot Coordination (ZSC) literature [4-5-27]. The search space for effective cooperative rewards requires synchronizing multi-agent incentives and utilizing robust algorithms like MAPPO [15].

Our work structurally diverges from this prior literature in two critical dimensions: First, we employ an objective-grounded selection mechanism, ensuring candidates are promoted based strictly on the original sparse mission objective rather than the shaped return, thereby preventing proxy optimization. Second, we integrate incentive diagnostic feedback, moving beyond scalar performance metrics to provide the LLM with structured insights into action coupling and multi-agent workload distribution.

3 Method

The general architecture of the proposed methodology is illustrated in fig. 1. The framework establishes an iterative reward engineering cycle that uniquely integrates the generative reasoning of LLMs with the rigorous evaluative mechanics of MARL. The architecture is initialized by a precise task description, while the LLM simultaneously leverages context retrieved from an archive to fully incorporate the history of previous reward attempts.

From this contextual foundation, the LLM synthesizes a set of K reward candidates. To guarantee computational viability and actively mitigate exploitable proxy behaviors, a formal validity envelope strictly constrains every generated program. These validated candidates then drive the training of multi-agent policies from scratch, utilizing a standard MAPPO baseline under a predefined computational budget.

Following the training phase, each candidate undergoes a rigorous evaluation based on the sparse task objective. After selecting the top-performing reward programs, a custom diagnostic feedback engine comprehensively analyzes the training rollouts. This engine extracts high-fidelity structured feedback that specifically quantifies action coupling, incentive alignment, and payoff balance. By integrating these diagnostic metrics with a dynamically updated archive, the framework systematically directs the LLM to synthesize the next generation of reward candidates (g). Ultimately, this closed-loop refinement enables the framework to autonomously discover increasingly sophisticated shaping signals, effectively bridging the gap between sparse feedback and robust cooperative coordination.

3.1 Problem Setting and Reward Interfaces

We consider a cooperative Markov game [3] defined by the tuple $\mathcal{G} = \langle \mathcal{S}, \{\mathcal{A}_i\}_{i=1}^n, \mathbf{P}, r_{\text{sparse}}, \gamma \rangle$, with n agents interacting within the state space \mathcal{S} . At each time step t , the environment is in state $s_t \in \mathcal{S}$. Each agent $i \in \{1, \dots, n\}$ selects an action $a_{t,i}$ from its individual action space \mathcal{A}_i , forming a joint action $\mathbf{a}_t = (a_{t,1}, \dots, a_{t,n}) \in \mathcal{A}$, where \mathcal{A} is the joint action space. The system dynamics follow the transition probability kernel $\mathbf{P} : \mathcal{S} \times \mathcal{A} \times \mathcal{S} \rightarrow [0, 1]$, which defines the probability $\mathbf{P}(s_{t+1} | s_t, \mathbf{a}_t)$ of transitioning to state s_{t+1} given the current state s_t and joint action \mathbf{a}_t . Furthermore, $r_{\text{sparse}} : \mathcal{S} \times \mathcal{A} \rightarrow \mathbb{R}$ defines the reward function for shared sparse tasks, and $\gamma \in [0, 1]$ is the discount factor.

In this cooperative setting, the task reward is sparse and shared; specifically, a scalar reward $r_{\text{sparse},t} = r_{\text{sparse}}(s_t, \mathbf{a}_t)$ is produced by the environment and assigned equally to all agents. The performance objective is to maximize the expected discounted sparse return:

$$J(\pi) = \mathbb{E}_{\tau \sim \pi} \left[\sum_{t=0}^{T-1} \gamma^t r_{\text{sparse},t} \right], \quad (1)$$

where π denotes the joint policy, τ represents a trajectory induced by π , and T is the episode horizon. In addition to the sparse reward, the simulator exposes structured instrumentation through an information record info_t . A deterministic feature map ϕ is used to convert the transition and instrumentation into a feature vector,

$$\mathbf{x}_t = \phi(s_t, \mathbf{a}_t, s_{t+1}, \text{info}_t). \quad (2)$$

A reward candidate is represented as an executable program p that produces agent-specific shaping signals from the instrumentation. Given the state features \mathbf{x}_t and the global sparse task reward $r_{\text{sparse},t}$, the program generates a vector of auxiliary shaping

$$\mathbf{r}_t^{(p)} = p(\mathbf{x}_t, r_{\text{sparse},t}) \in \mathbb{R}^n, \quad (3)$$

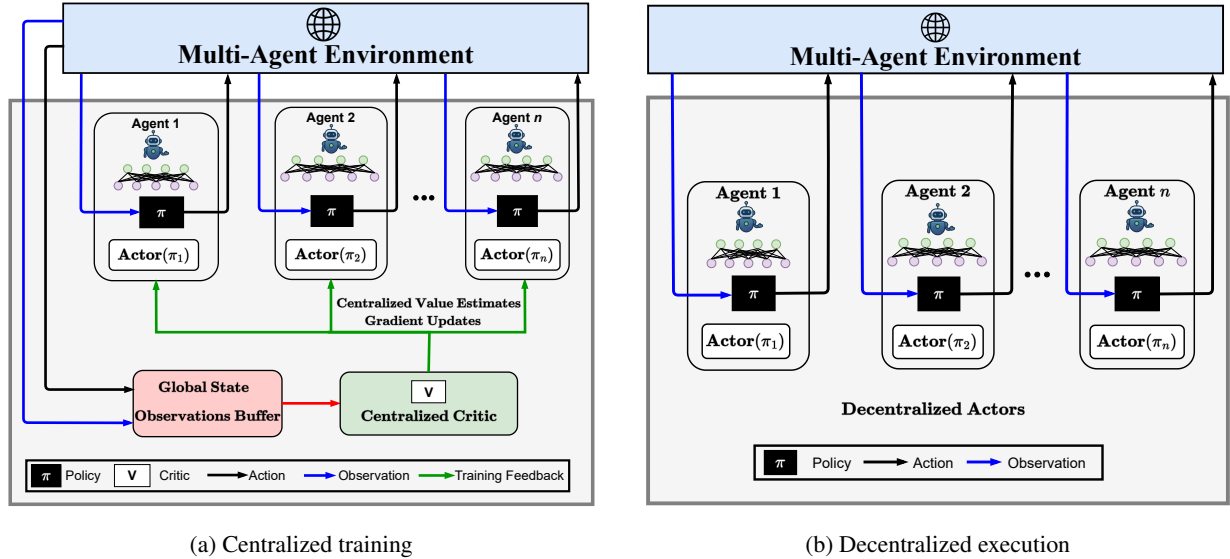


Figure 2: Overview of the CTDE paradigm for multi-agent reinforcement learning. (a) Centralized training: a shared critic (V) utilizes global state information and joint observation buffers to guide policy updates via training feedback. (b) Decentralized execution: individual actors (π_i) rely exclusively on local observations for action selection, ensuring scalability in partially observable environments.

where the i -th component $r_{t,i}^{(p)}$ denotes the shaping signal assigned to agent i at step t . During training, each agent receives an augmented reward

$$\tilde{r}_{t,i} = r_{\text{sparse},t} + \lambda r_{t,i}^{(p)}, \quad (4)$$

where $\lambda \geq 0$ is the fixed scaling factor. The sparse reward term preserves the intended task objective, while the shaping term is used only to improve learning under finite budgets. In all results reported, the candidates are compared using the sparse objective in eq. (1), not the shaped return.

3.2 Objective-Grounded Search and Selection

Let $\text{Train}(\cdot; \theta, \xi)$ denote training with a fixed MARL learner (MAPPO) using fixed hyperparameters θ and randomness ξ . The candidate evaluation process adheres to the centralized training decentralized execution (CTDE) paradigm, as illustrated in fig. 2. During the centralized training phase (fig. 2a), a centralized critic V leverages a shared buffer of global states and joint observations to evaluate the collective policy and derive training feedback. This centralized value estimate is utilized to provide advantage signals that guide the policy updates for all agents. Conversely, during the decentralized execution phase (fig. 2b), the decentralized actors π_i select actions based strictly on local observations. Upon completion of training with the augmented rewards defined in eq. (4), the candidate is evaluated exclusively via the sparse task objective \mathcal{G} to obtain the empirical estimate $\hat{J}(p)$.

The search process evolves over a total of G generations. At each generation index $g \in \{1, \dots, G\}$, a structured context c_g is constructed from the task description, the instrumentation schema, the reward interface, and summaries of previously evaluated candidates. The LLM proposes K reward candidates by sampling from a conditional distribution $q_\psi(p | c_g)$. Each candidate p is filtered by a validity envelope before training. The envelope enforces correct input and output signatures, determinism, bounded outputs via clipping, and robustness to missing instrumentation keys. Candidates failing validation are rejected, and when failures are syntactic or runtime in nature, a bounded number of repair attempts are performed by conditioning on the error trace.

Within each generation, candidates are trained and evaluated, and the best candidate is selected based on the sparse return:

$$p_g^* \in \arg \max_{k \in \mathcal{V}_g} \hat{J}(p_{g,k}), \quad (5)$$

where $p_{g,k}$ is the k -th candidate in generation g for $k \in \mathcal{V}_g \subseteq \{1, \dots, K\}$, and \mathcal{V}_g denotes the set of indices for candidates that pass validation. Selection is objective-grounded because only the sparse return is used for promotion. The complete procedure, which encompasses LLM-based iterative reward generation and the MARL evaluation loop, is summarized in algorithm 1.

Algorithm 1: Objective-grounded incentive-aware reward search.

Require : Task specification and instrumentation schema; validity envelope; learner settings θ ; generations G ; candidates per generation K

```

1 Initialize archive  $\mathcal{A} \leftarrow \emptyset$ , and best score  $\hat{J}_{\text{best}} \leftarrow -\infty$ 
2 for  $g = 1$  to  $G$  do
3   Construct context  $c_g$  from task description and archive summaries
4   Sample candidates  $\{p_{g,k}\}_{k=1}^K \sim q_\psi(p | c_g)$ 
5   for  $k = 1$  to  $K$  do
6     Validate and, if needed, repair  $p_{g,k}$ 
7     if  $p_{g,k}$  is valid then
8       Train policy  $\pi_{g,k} \leftarrow \text{Train}(\cdot; \theta, \xi)$  using augmented rewards  $\tilde{r}_{t,i}$ 
9       Evaluate estimate  $\hat{J}(p_{g,k})$  using sparse reward only
10      Compute diagnostics  $d(p_{g,k})$  from rollouts
11       $\mathcal{A} \leftarrow \mathcal{A} \cup \{(p_{g,k}, \hat{J}(p_{g,k}), d(p_{g,k}))\}$ 
12    end if
13  end for
14  Update context summaries in  $\mathcal{A}$ 
15 end for
Return : Best candidate  $p^* = \arg \max_{(p, \cdot) \in \mathcal{A}} \hat{J}(p)$ 

```

3.3 Incentive Diagnostics Used for Feedback

The candidate program can assign different shaping signals to different agents, even when the task objective is shared. For interpretability, the shaping component is analyzed separately from the sparse reward. Using the agent-specific shaping signal $r_{t,i}^{(p)}$, the discounted shaping return for agent i on a rollout is defined as:

$$S_i(p) = \sum_{t=0}^{T-1} \gamma^t r_{t,i}^{(p)}. \quad (6)$$

These returns are computed on the shaping component only and therefore can be asymmetric even when the environment reward is a shared team reward.

3.3.1 Payoff imbalance.

Payoff imbalance measures the disparity in shaping returns across n agents. To ensure the metric remains bounded and interpretable, we define it as the normalized sum of all-pairs differences:

$$\Delta(p) = \frac{\sum_{i=1}^n \sum_{j=i+1}^n |S_i(p) - S_j(p)|}{(n-1) \sum_{k=1}^n |S_k(p)| + \varepsilon}, \quad (7)$$

where $\varepsilon > 0$ is a small constant for numerical stability. This formulation is bounded within $[0, 1]$, where $\Delta(p) \rightarrow 0$ indicates a symmetric distribution of rewards and larger values signal a disproportionate concentration on a subset of agents.

3.3.2 Incentive alignment

Incentive alignment measures the degree to which per-step shaping signals concurrently reinforce the agents. For an ensemble of n agents, we define this as the average pairwise Pearson correlation across all time steps in an episode:

$$\rho(p) = \frac{2}{n(n-1)} \sum_{i=1}^n \sum_{j=i+1}^n \text{corr} \left(r_{t,i}^{(p)}, r_{t,j}^{(p)} \right). \quad (8)$$

Strongly positive values ($\rho \rightarrow 1$) indicate that the shaping signals are synchronized, suggesting that the reward program p induces mutually reinforcing behaviors. Conversely, values near zero or negative suggest decoupled or conflicting incentives, potentially signaling a breakdown in cooperative dynamics or the optimization of competitive proxy goals.

3.3.3 Action Coupling

Action coupling quantifies the statistical dependence between the agents’ decision-making processes under the policy optimized via program p . For an ensemble of n agents, we report the average pairwise Normalized Mutual Information (NMI) across all time steps:

$$\text{NMI}(p) = \frac{2}{n(n-1)} \sum_{i=1}^n \sum_{j=i+1}^n \frac{I(A_i; A_j)}{\sqrt{H(A_i)H(A_j)}}, \quad (9)$$

where $I(A_i; A_j)$ denotes the mutual information between the action distributions of agents i and j , and $H(A_i)$ represents the marginal entropy of the discrete action random variable A_i estimated from rollout data. Unlike raw mutual information, this geometric mean normalization ensures the metric is bounded within $[0, 1]$, where higher NMI indicates more interdependent action selection. This serves as a proxy for identifying whether the synthesized reward signals induce emergent coordination or lead to independent, decoupled strategies.

Upon the completion of each evaluation rollout, the framework logs a comprehensive diagnostic tuple for every candidate:

$$d(p) = \left(\hat{J}(p), \Delta(p), \rho(p), \text{NMI}(p) \right), \quad (10)$$

which characterizes the candidate’s performance, payoff distribution, signal alignment, and behavioral coupling, respectively. While these diagnostics serve as high-dimensional descriptive feedback to guide the LLM proposer in subsequent generations, the final selection and promotion mechanism remains strictly exclusive to the sparse task return $\hat{J}(p)$. This decoupling ensures that while the search process is informed by complex coordination metrics, the optimization objective remains grounded in the true environment goal, preventing the emergence of reward-hacking or the optimization of unintended proxy behaviors.

4 Results

In this section, we evaluate the effectiveness of our diagnostic-grounded reward search to discover rewards that strengthen multi-agent coordination. We first introduce the benchmark layouts and the specific coordination challenges inherent in each. Next, we detail the training protocol used to evaluate the generated rewards. We then analyze the objective performance gains across successive generations and highlight the learning dynamics in environments characterized by significant interaction bottlenecks. Finally, we provide a detailed diagnostic analysis to clarify how the discovered shaping signals influence agent interdependence, incentive alignment, and payoff distribution.

4.1 Layout Characteristics and Coordination Challenges

Evaluation is conducted within the Overcooked-AI cooperative cooking environment [4], a benchmark requiring a pair of agents ($n = 2$) to coordinate navigation, resource management, and precise temporal handoffs to deliver completed soups. Formally, at each timestep, the agents receive a state representation encoding the spatial layout and the status of all entities, including agent positions, ingredients, cooking pots, and serving counters. Both agents operate within a shared, discrete action space consisting of six actions: moving in four cardinal directions (*up*, *down*, *left*, *right*), taking no action (*stay*), and *interacting* with objects. Each episode runs for a fixed horizon of $H = 200$ timesteps. True to the sparse reward setting, the environment yields a joint task reward (typically +20) only upon the successful delivery of a completed soup, with zero intermediate environmental rewards provided for sub-tasks.

We evaluate our framework across four layouts, each representing a distinct point on the spectrum of dyadic coordination challenges (see fig. 3). Cramped Room (fig. 3a) serves as a dense, shared workspace where agents must navigate narrow corridors and mitigate spatial contention. Forced Coordination (fig. 3b) physically decouples key resources, making progress strictly dependent on repeated handoffs and synchronized turn-taking. Coordination Ring (fig. 3c) focuses on

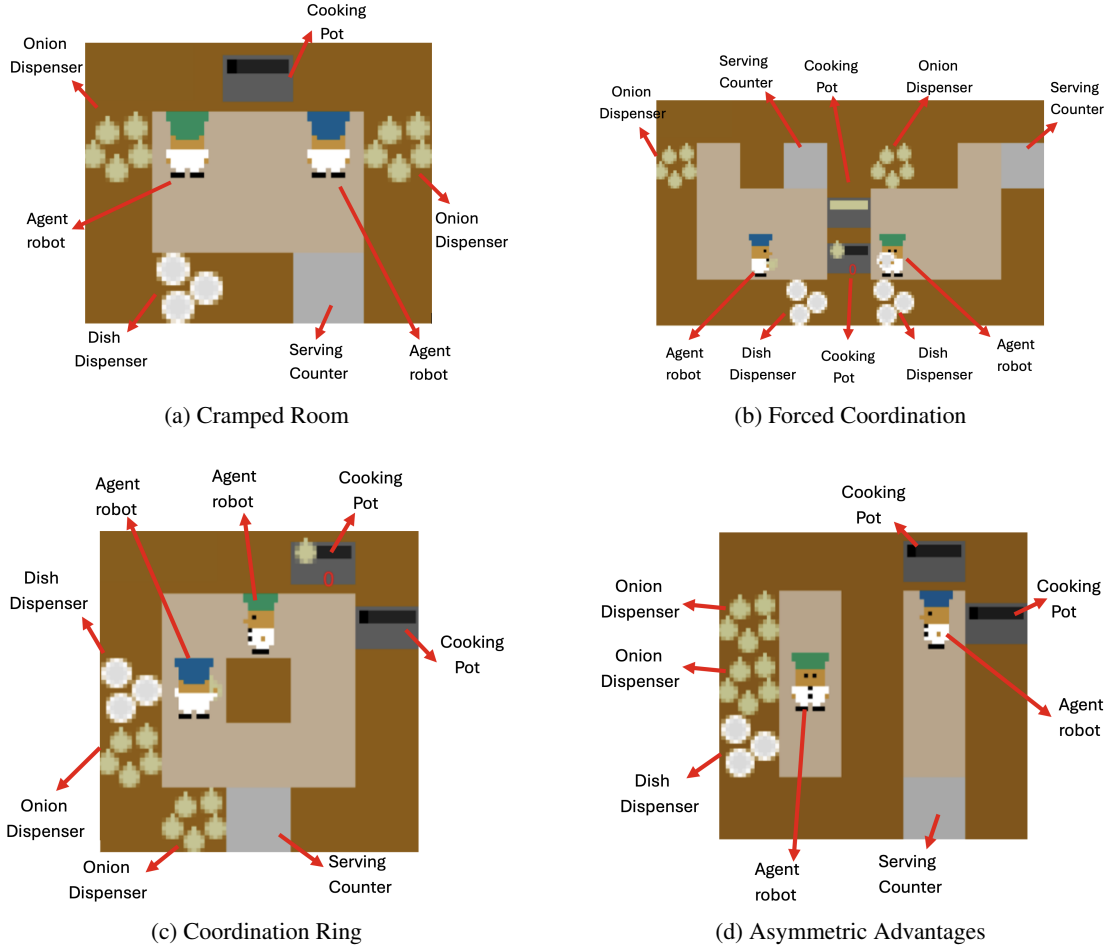


Figure 3: Overcooked-AI layouts and coordination challenges. Each environment isolates specific facets of multi-agent cooperation: (a) Cramped Room evaluates spatial efficiency and collision avoidance in shared workspaces. (b) Forced Coordination necessitates strict functional specialization and inter-agent hand-offs. (c) Coordination Ring tests movement synchronization to prevent bottlenecks in circular corridors. (d) Asymmetric Advantages introduces resource-specific disparities, requiring strategic role delegation based on proximity to dispensers.

Table 1: Fixed MAPPO Hyperparameters used for candidate evaluation.

Hyperparameter	Value
Actor Learning Rate	5×10^{-4}
Critic Learning Rate	1×10^{-3}
Discount Factor (γ)	0.99
GAE Parameter (α)	0.95
PPO Clip Ratio	0.2
Entropy Coefficient	0.01
Minibatch Size	256
Optimization Epochs	10
Network Architecture	2-layer MLP (64, 64)
Activation Function	ReLU

high-level movement synchronization within a circular topology; here, sparse feedback makes deadlocks and mistimed detours particularly detrimental to joint performance. Finally, Asymmetric Advantages (fig. 3d) introduces structural disparities in access paths and staging zones, necessitating the emergence of complementary roles to achieve compatible joint execution.

4.2 Training Protocol

The proposed framework iteratively refines reward structures across $G = 2$ generations. In each generation, the LLM synthesizes $K = 4$ candidate reward functions based solely on the task specifications. To evaluate the viability of these candidates, we employ a MAPPO baseline to train the agents. For computational efficiency, each candidate undergoes a rapid evaluation phase consisting of exactly 21 iterations in the training. Throughout this phase, the underlying environment dynamics remain constant, with every episode strictly terminating at the predefined horizon of $H = 200$ timesteps.

Upon the completion of the 21 iterations, the diagnostic engine extracts behavioral metrics and payoff distributions. This data acts as structured feedback for the LLM, prompting the second generation ($G = 2$) of reward synthesis to correct observed coordination gaps, such as deadlocks or asymmetric pacing. We train all agents using the MAPPO algorithm with the hyperparameters presented in table 1.

4.3 Objective Performance and Learning Dynamics

The empirical success of the diagnostic-grounded search is demonstrated by the progression of the sparse task return J across two successive generations. As reported in table 2, each search generation is executed using a MAPPO baseline, where candidates are trained from the scratch under a fixed computational budget and selected exclusively based on the sparse task objective.

Across all evaluated layouts, we observe a consistent monotonic increase in both sparse returns and successful delivery counts in later generations. The most substantial gains are realized in Coordination Ring and Forced Coordination, where baseline performance is severely constrained by the difficulty of credit assignment under tight interaction bottlenecks. In these scenarios, the baseline agents frequently suffers from coordination failures such as deadlocks, mistimed passing, and handoff synchronization issues.

The synthesized reward programs from later generations effectively bridge this exploration gap by providing dense auxiliary signals for intermediate progress. This acceleration in coordination discovery is clearly reflected in the results: for instance, in the Coordination Ring layout, the Generation (Gen) 2 candidate achieves a nearly 12-fold increase in successful deliveries compared to the baseline (7.65 vs. 0.15), while simultaneously reducing invalid deliveries from 11.30 to 0.85. In more straightforward layouts like Cramped Room and Asymmetric Advantages, where the baseline performance is naturally stronger, the framework continues to yield incremental but statistically significant improvements within the same compute budget.

The temporal evolution of agent performance across the four evaluation layouts, illustrated by the learning curves in fig. 4, underscores the critical role of synthesized rewards in accelerating coordination. In relatively straightforward environments such as Cramped Room (fig. 4a), all candidates eventually surpass the baseline. However, the Gen 2 candidate demonstrates significantly higher sample efficiency and achieves the baseline final performance level in nearly half the iterations. This trend highlights the superior learning speed provided by the refined reward signals. In contrast, Forced Coordination (fig. 4b) presents a strict coordination bottleneck where agents must synchronize their actions to pass ingredients. While the MAPPO baseline struggles with high variance and often fails to break the zero-reward barrier early in training, the Gen 2 candidate shows a consistent upward trajectory. This confirms that the diagnostic feedback effectively addressed the synchronization issues inherent in this layout.

The most challenging scenario for the baseline is observed in Coordination Ring (fig. 4c), where performance remains almost entirely flat throughout the training process. Here, the transition from Gen 1 to Gen 2 represents a qualitative breakthrough. While Gen 1 begins to explore successful strategies, Gen 2 fully exploits the dense diagnostic rewards to achieve a robust and high-performing policy. This effectively solves a task where standard MAPPO fails to converge.

Table 2: Final evaluation on four Overcooked layouts. J denotes sparse return (mean \pm std across evaluation episodes). Deliveries and invalid deliveries are episode means.

Layout	J			Deliveries			Invalid Deliveries		
	Baseline	Gen 1	Gen 2	Baseline	Gen 1	Gen 2	Baseline	Gen 1	Gen 2
Cramped Room	148 \pm 39	180 \pm 25	188 \pm 10	7.40	9.00	9.40	1.15	0.25	0.75
Forced Coordination	32 \pm 14	55 \pm 26	103 \pm 29	1.60	2.75	5.15	0.80	1.25	0.30
Coordination Ring	13 \pm 5	102 \pm 28	153 \pm 24	0.15	5.10	7.65	11.30	3.50	0.85
Asymmetric Advantages	231 \pm 38	322 \pm 36	381 \pm 25	11.55	16.10	19.05	6.15	3.45	1.55

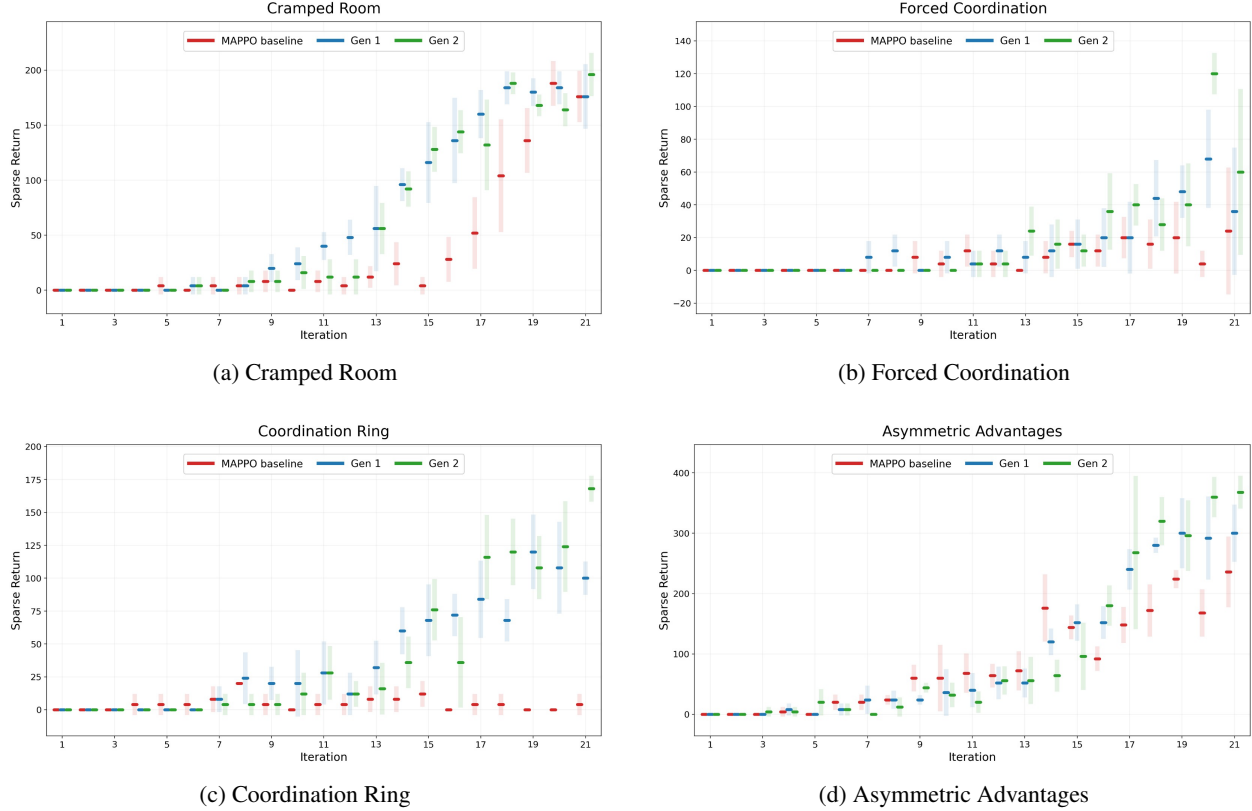


Figure 4: Learning curves of evaluation sparse return J . Performance comparison between the MAPPO baseline and the selected candidates from the first and second generations across four layouts: (a) Cramped Room, (b) Forced Coordination, (c) Coordination Ring, and (d) Asymmetric Advantages. Shaded regions indicate variability across evaluation episodes.

Finally, in Asymmetric Advantages (fig. 4d), although the baseline performs reasonably well through the use of simple roles, the Gen 2 candidate reaches a substantially higher final performance level. The notably reduced variance in the Gen 2 curve further suggests that the synthesized rewards provide a more stable learning process. This leads to more predictable and reliable agent behavior compared to the inconsistent nature of the baseline. Collectively, these results empirically validate that our framework not only improves final performance but also consistently accelerates the discovery of complex multi-agent coordination. Most importantly, the observed monotonic progression from the baseline to Gen 2 across all layouts confirms the robustness of the diagnostic-grounded search. It demonstrates that each successive generation of our framework successfully refines the reward structures to achieve higher task success and improved learning stability.

To further elucidate the search process, fig. 5 provides a structural lineage of candidate promotion across generations. Each node represents an independent training run of a synthesized reward program, while edges indicate the genealogical path used to condition subsequent LLM prompts. This hierarchical selection mechanism ensures that the search space is effectively pruned toward objective-aligned regions.

The lineage diagrams highlight a robust compounding effect in all environments. For instance, in Forced Coordination, the jump from the Baseline (32 ± 14) to Gen 2 (103 ± 29) is not merely a result of chance. It is the outcome of a structured refinement process in which successful shaping strategies from the first generation serve as a foundation for more complex incentives in the second. This iterative improvement confirms that the LLM agent successfully interprets the diagnostic feedback from previous iterations. This process mitigates coordination bottlenecks, such as deadlocks and synchronization failures, which otherwise impede the baseline learner. Furthermore, the promotion paths demonstrate that the framework consistently identifies and builds upon the most promising reward structures, which leads to the significant performance gains observed in the final generation.

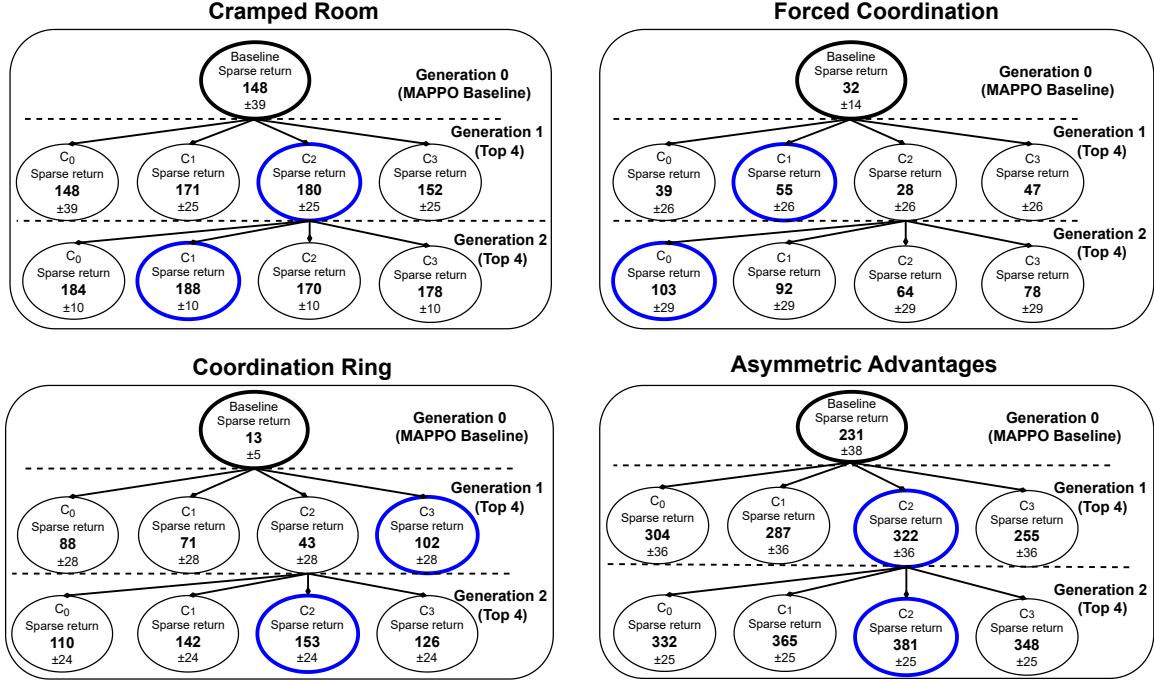


Figure 5: Candidate promotion diagram. Nodes summarize evaluated candidates and objective scores, and edges indicate the promotion path used to condition subsequent generations.

4.4 Coordination Diagnostics and Interaction Patterns

The incentive diagnostics clarify the evolution of interaction patterns and shaping signals across generations. These quantities represent descriptive summaries from actual training rollouts. They do not represent claims about theoretical equilibrium states or final convergence points. Instead, these metrics reflect the practical behavior of the agents during their interactions. Payoff imbalance and incentive alignment calculations focus on the candidate shaping component rather than the shared sparse task reward. Consequently, these metrics capture how the auxiliary learning signal is distributed among the agents. fig. 6 shows the mean diagnostic values for candidate pools that satisfy a minimum sparse-return criterion. The results highlight two key findings.

First, the action coupling, measured through Normalized Mutual Information (NMI), increases across successive search generations in all layouts (fig. 6a-d). This trend indicates that high-performance reward candidates facilitate more interdependent action selection. In the Overcooked environment, effective performance relies on precise coordinated timing and mutual adaptation. This requirement includes corridor yield maneuvers, the sequencing of interactions at shared stations, and the synchronization of travel paths. The observed increase in NMI reflects the emergence of these strategic dependencies, as agents learn to condition their policies more tightly on the actions of their partners.

Second, incentive alignment (ρ) increases in Cramped Room, Coordination Ring, and Asymmetric Advantages (fig. 6a, c, d). This result indicates that the proposed shaping signals for both agents exhibit a higher positive correlation in later generations. In practice, this pattern aligns with shaping programs that reinforce intermediate progress toward shared subgoals. This alignment prevents the introduction of competing gradients that might destabilize coordination. Instead, the reward structures ensure that individual improvements contribute directly to the collective objective.

A layout-specific pattern is evident in Forced Coordination (fig. 6b). Because this layout depends on repeated handoffs, the shaping that concentrates auxiliary return on a single agent can create asymmetric learning dynamics. In such cases, one agent receives strong gradients while the other receives weak or noisy guidance. The payoff imbalance diagnostic (Δ) decreases significantly between generations in Forced Coordination (fig. 6b). This indicates a more uniform distribution of shaping signals for the selected later-generation candidates. This behavior remains consistent with reward programs that provide guidance for both roles necessary for successful handoffs and demonstrates that the search process successfully identifies incentives that balance the learning signal, which leads to the robust coordination observed in the final policies.

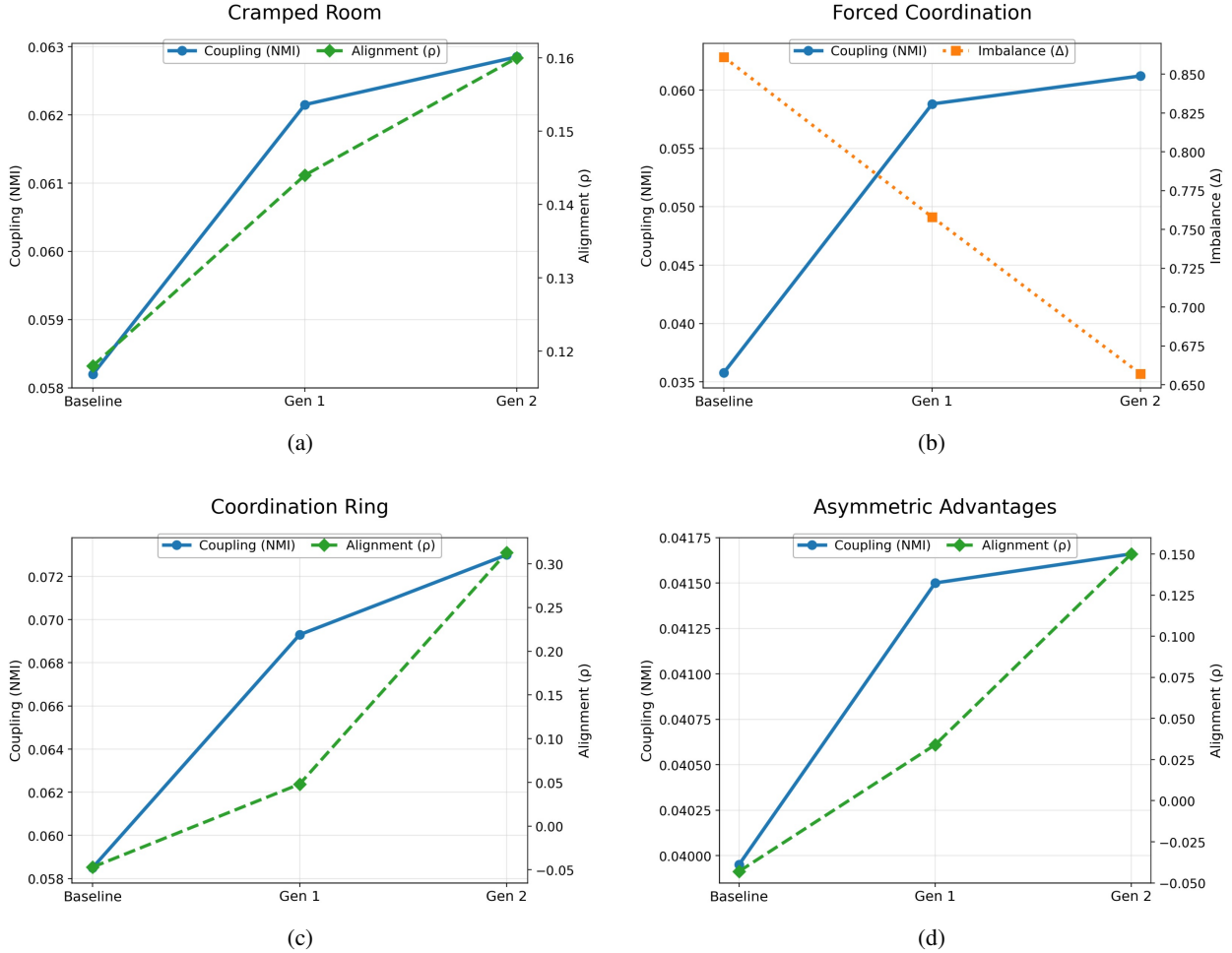


Figure 6: Empirical coordination diagnostics across Overcooked-AI layouts. (a) Cramped Room: action coupling (NMI) and incentive alignment (ρ) trends signify reduced collision rates. (b) Forced Coordination: decline in payoff imbalance (Δ) indicates equitable workload distribution. (c) Coordination Ring: growth in ρ and NMI demonstrates synchronized circular motion. (d) Asymmetric Advantages: NMI trajectory confirms specialized reward structures. The plots illustrate the iterative improvement from Baseline to Generation 2. Blue solid lines represent NMI, green dashed lines show ρ , and orange dotted lines indicate Δ .

5 Conclusion

An objective-grounded approach to autonomous reward program synthesis for cooperative MARL has been presented. In this framework, an LLM generates candidate shaping programs from environment instrumentation. These candidates remain constrained by a formal validity envelope and undergo evaluation under a fixed MAPPO learner. Selection across successive generations depends solely on the sparse task return; consequently, performance improvements relate directly to the intended objective rather than to the auxiliary shaping signal itself.

Across the four Overcooked-AI layouts, later search generations exhibit higher sparse returns and increased delivery counts. The most pronounced gains appear in the layouts that contain interaction bottlenecks under sparse feedback. Diagnostic trends for the shaping component indicate increased action coupling and higher alignment of shaping signals in coordination-heavy tasks. Furthermore, a reduction in the shaping concentration on a single agent is evident in handoff-driven layouts. These results suggest that objective-grounded reward program search can mitigate the burden of manual reward engineering. The proposed method also yields shaping signals compatible with stable cooperative learning under finite training budgets.

The success of this iterative search process demonstrates the potential for LLM-guided reward discovery in environments with complex coordination challenges. While the current study focuses on the Overcooked benchmark, the

principles of diagnostic-grounded synthesis remain applicable to broader classes of multi-agent coordination problems. Future research may extend this framework to large-scale multi-agent systems where reward programs must facilitate coordination among dozens of agents in continuous state spaces. Additionally, exploring the synthesis of rewards for heterogeneous collectives where agents possess differing capabilities and specialized roles could further validate the adaptability of diagnostic-grounded search in diverse industrial and logistics coordination tasks.

References

- [1] Richard S Sutton and Andrew G Barto. *Reinforcement learning: An introduction*. MIT press, 2018.
- [2] Jakob Foerster, Gregory Farquhar, Triantafyllos Afouras, Nantas Nardelli, and Shimon Whiteson. Counterfactual multi-agent policy gradients. In *Proceedings of the AAAI Conference on Artificial Intelligence*, volume 32, 2018.
- [3] Michael L. Littman. Markov games as a framework for multi-agent reinforcement learning. In *Proceedings of the Eleventh International Conference on Machine Learning (ICML)*, pages 157–163. Morgan Kaufmann, 1994.
- [4] Micah Carroll, Rohin Shah, Mark K. Ho, Tom Griffiths, Sanjit A. Seshia, Pieter Abbeel, and Anca D. Dragan. On the utility of learning about humans for human-ai coordination. In *Advances in Neural Information Processing Systems (NeurIPS)*, pages 5175–5186, 2019.
- [5] Hengyuan Hu, Adam Lerer, Alex Peysakhovich, and Jakob Foerster. “Other-play” for zero-shot coordination. In *International Conference on Machine Learning (ICML)*, pages 4399–4410. PMLR, 2020.
- [6] Andrew Y. Ng, Daishi Harada, and Stuart J. Russell. Policy invariance under reward transformations: Theory and application to reward shaping. In *Proceedings of the Sixteenth International Conference on Machine Learning (ICML)*, pages 278–287. Morgan Kaufmann, 1999.
- [7] Sam Devlin, Logan Yliniemi, Daniel Kudenko, and Kagan Tumer. Potential-based difference rewards for multiagent reinforcement learning. In *Proceedings of the 13th International Conference on Autonomous Agents and Multiagent Systems (AAMAS)*, pages 165–172, 2014.
- [8] Brian D. Ziebart, Andrew Maas, J. Andrew Bagnell, and Anind K. Dey. Maximum entropy inverse reinforcement learning. In *Proceedings of the Twenty-Third AAAI Conference on Artificial Intelligence (AAAI)*, pages 1433–1438, 2008.
- [9] Paul F. Christiano, Jan Leike, Tom B. Brown, Miljan Martic, Shane Legg, and Dario Amodei. Deep reinforcement learning from human preferences. In *Advances in Neural Information Processing Systems (NeurIPS)*, 2017.
- [10] Ashish Vaswani, Noam Shazeer, Niki Parmar, Jakob Uszkoreit, Llion Jones, Aidan N. Gomez, Łukasz Kaiser, and Illia Polosukhin. Attention is all you need. In *Advances in Neural Information Processing Systems (NeurIPS)*, 2017.
- [11] Tom B. Brown, Benjamin Mann, Nick Ryder, Melanie Subbiah, Jared Kaplan, Prafulla Dhariwal, Arvind Neelakantan, Pranav Shyam, Girish Sastry, Amanda Askell, Ariel Herbert-Voss, Gretchen Krueger, Tom Henighan, Rewon Child, Aditya Ramesh, Daniel Ziegler, Jeffrey Wu, Clemens Winter, Christopher Hesse, Mark Chen, Eric Sigler, Mateusz Litwin, Scott Gray, Benjamin Chess, Jack Clark, Christopher Berner, Sam McCandlish, Alec Radford, Ilya Sutskever, and Dario Amodei. Language models are few-shot learners. In *Advances in Neural Information Processing Systems (NeurIPS)*, 2020.
- [12] Yujia Li, David Choi, Junyoung Chung, et al. Competition-level code generation with AlphaCode. *Science*, 378(6624):1092–1097, 2022.
- [13] Yecheng Jason Ma, William Liang, Guanzhi Wang, De-An Huang, Osbert Bastani, Dinesh Jayaraman, Yuke Zhu, Linxi Fan, and Anima Anandkumar. EUREKA: Human-level reward design via coding large language models. In *International Conference on Learning Representations (ICLR)*, 2024.
- [14] Tianbao Xie, Siheng Zhao, Chen Henry Wu, Yitao Liu, Qian Luo, Victor Zhong, Yanchao Yang, and Tao Yu. Text2reward: Reward shaping with language models for reinforcement learning. In *International Conference on Learning Representations (ICLR)*, 2024.
- [15] Chao Yu, Akash Velu, Eugene Vinitsky, Jiaxuan Gao, Yu Wang, Alexandre Bayen, and YI WU. The surprising effectiveness of ppo in cooperative multi-agent games. In S. Koyejo, S. Mohamed, A. Agarwal, D. Belgrave, K. Cho, and A. Oh, editors, *Advances in Neural Information Processing Systems*, volume 35, pages 24611–24624. Curran Associates, Inc., 2022.
- [16] Dylan Hadfield-Menell, Smitha Milli, Pieter Abbeel, Stuart Russell, and Anca Dragan. Inverse reward design. In *Advances in Neural Information Processing Systems (NeurIPS)*, 2017.

- [17] Anna Harutyunyan, Sam Devlin, Peter Vrancx, and Ann Nowé. Expressing arbitrary reward functions as potential-based advice. In *Proceedings of the Twenty-Ninth AAAI Conference on Artificial Intelligence (AAAI)*, pages 2652–2658, 2015.
- [18] Sam Devlin and Daniel Kudenko. Theoretical considerations of potential-based reward shaping for multi-agent systems. In *Proceedings of the Tenth International Conference on Autonomous Agents and Multiagent Systems (AAMAS)*, 2011.
- [19] Tabish Rashid, Mikayel Samvelyan, Christian Schroeder de Witt, Gregory Farquhar, Jakob Foerster, and Shimon Whiteson. Monotonic value function factorisation for deep multi-agent reinforcement learning. *Journal of Machine Learning Research*, 21(178):1–51, 2020.
- [20] Peter Sunehag, Guy Lever, Audrunas Gruslys, Wojciech Marian Czarnecki, Vinicius Zambaldi, Max Jaderberg, Marc Lanctot, Nicolas Sonnerat, Joel Z. Leibo, Karl Tuyls, and Thore Graepel. Value-decomposition networks for cooperative multi-agent learning based on team reward. In *Proceedings of the 17th International Conference on Autonomous Agents and MultiAgent Systems*, page 2085–2087, Richland, SC, 2018. International Foundation for Autonomous Agents and Multiagent Systems.
- [21] Sam Devlin, Marek Grześ, and Daniel Kudenko. An empirical study of potential-based reward shaping and advice in complex, multi-agent systems. *Advances in Complex Systems*, 14(2):251–278, 2011.
- [22] Andrew Y. Ng and Stuart J. Russell. Algorithms for inverse reinforcement learning. In *Proceedings of the Seventeenth International Conference on Machine Learning, ICML '00*, page 663–670, San Francisco, CA, USA, 2000. Morgan Kaufmann Publishers Inc.
- [23] Nisan Stiennon, Long Ouyang, Jeff Wu, Daniel M. Ziegler, Ryan Lowe, Chelsea Voss, Alec Radford, Dario Amodei, and Paul Christiano. Learning to summarize from human feedback. In *Proceedings of the 34th International Conference on Neural Information Processing Systems, NIPS '20*, Red Hook, NY, USA, 2020. Curran Associates Inc.
- [24] David H. Wolpert and Kagan Tumer. Collective intelligence, data routing and braess' paradox. *Journal of Artificial Intelligence Research*, 16:359–387, 2002.
- [25] Chengrun Yang, Xuezhi Wang, Yifeng Lu, Hanxiao Liu, Quoc V Le, Denny Zhou, and Xinyun Chen. Large language models as optimizers. In *International Conference on Learning Representations (ICLR)*, 2024.
- [26] Martin Klissarov, Pierluca D'Oro, Shagun Sodhani, Roberta Raileanu, Pierre-Luc Bacon, Pascal Vincent, Amy Zhang, and Mikael Henaff. Motif: Intrinsic motivation from artificial intelligence feedback. In *The Twelfth International Conference on Learning Representations*, 2024.
- [27] DJ Strouse, Kevin R. McKee, Matt Botvinick, Edward Hughes, and Richard Everett. Collaborating with humans without human data. NIPS '21, Red Hook, NY, USA, 2021. Curran Associates Inc.